Covalent Catalysis by Pyridoxal: Evaluation of the Effect of the Cofactor on the Carbon Acidity of Glycine

ARTICLE *in* JOURNAL OF THE AMERICAN CHEMICAL SOCIETY · APRIL 2007

Impact Factor: 12.11 · DOI: 10.1021/ja0679228 · Source: PubMed

Published in final edited form as:
J Am Chem Soc. 2007 March 14; 129(10): 3013–3021. doi:10.1021/ja0679228.

Covalent Catalysis by Pyridoxal:

Evaluation of the Effect of the Cofactor on the Carbon Acidity of Glycine

Krisztina Toth and **John P. Richard**
Department of Chemistry, University at Buffalo, SUNY, Buffalo, New York 14260

Abstract

First-order rate constants for deprotonation of the α-imino carbon of the adduct between 5′-deoxypyridoxal (**1**) and glycine were determined as the rate constants for Claisen-type addition of glycine to **1** where deprotonation is rate determining for product formation. There is no significant deprotonation at pH 7.1 of the form of the **1**-glycine iminium ion with the pyridine nitrogen in the basic form. The value of k_{HO} for hydroxide ion-catalyzed deprotonation of the α-imino carbon increases from 7.5×10^2 to 3.8×10^5 to 3.0×10^7 M^{-1} s^{-1}, respectively, with protonation of the pyridine nitrogen, the phenoxide oxyanion and the carboxylate anion of the **1**-glycine iminium ion. There is a corresponding decrease in the pK_as for deprotonation of the α-imino carbon from 17 to 11 to 6. It is proposed that enzymes selectively bind and catalyze the reaction of the iminium ion with pK_a = 17. A comparison of $k_B = 1.7 \times 10^{-3}$ s^{-1} for deprotonation of the α-imino carbon of this cofactor-glycine adduct (pK_a = 17 by HPO_4^{2-} with $k_{cat}/K_m = 4 \times 10^5 M^{-1}$ s^{-1} for catalysis of amino-acid racemization by alanine racemase shows that the enzyme causes a *ca* 2×10^8-fold acceleration of the rate of deprotonation the α-imino carbon. This corresponds to about one-half of the burden borne by alanine racemase in catalysis of deprotonation of alanine.

Introduction

Enzymes accelerate deprotonation of the α-amino carbon of amino acids by providing an environment favorable for deprotonation of the bound substrate[1-5] and/or through covalent modification that increases the carbon acidity of the amino acid.[6,7] We are interested in determining the effect of such covalent modifications on the carbon acid pK_a of ≈ 34 for the simple amino acid glycine[8,9] and have shown that this pK_a is decreased to 14 through systematic modification of the amino and carboxylate groups of glycine (Chart 1).[8-10] Pyridoxal 5′-phosphate (Scheme 1) is an extraordinary electrophilic catalyst of carbon deprotonation of α-amino acids in solution and in a number of enzymatic reactions for which it is serves as a cofactor. The first step in the mechanism for covalent catalysis by PLP is formation of an imine between the amino acid and PLP. Formation of this adduct labilizes all of the bonds of the α-imino carbon, because heterolytic bond cleavage with loss of H^+, CO_2 or R^+ gives an enolate that is strongly stabilized by delocalization of negative charge onto the pyridine ring of the cofactor (Scheme 1).

Despite extensive studies to characterize covalent catalysis by PLP in enzymatic[11-16] and model reactions,[17-22] there are no modern estimates of the carbon acid pK_a(s) of the key iminium ion intermediate of these reactions. For example, it was stated recently that there is

jrichard@chem.buffalo.edu.

Supporting Information Available: Table of observed first order rate constants (k_{obsd}) for Claisen-type addition of glycine to **1** under reaction conditions where deprotonation of **2** is rate determining for product formation (Scheme 2). This material is available free of charge via the Internet at http://pubs.acs.org.

"no available experimental information on the energies of the carbanionic intermediate for the uncatalyzed or PLP catalyzed reactions (or on their existence)".[23] The kinetic barriers determined in elegant studies by Bruice and coworkers for racemization of alanine catalyzed by a PLP analog provide insight into the kinetic barrier for carbon deprotonation of the iminium ion reaction intermediate,[17-19] and these barriers have been estimated in recent computational studies by Gao and coworkers.[24] However, the effect of formation of an iminium ion between PLP and simple amino acids on the pK_a of 34 for deprotonation of glycine has not been examined within the framework of recent advances in the evaluation of substituent effects on carbon acidity.

We recently reported that the reaction of the pyridoxal analog 5′-deoxypyridoxal (**1**) and glycine gives the Claisen-type adduct **4** as the only detectable product over 4-halftimes for the reaction of **1** (Scheme 2).[25] The rate determining step for this reaction at pH 2 - 7 is deprotonation of the glycine iminium ion ($k_p = k_{HO}$[HO] + k_B[B], Scheme 2), because addition of **1** to the resulting pyridoxal-stabilized glycine carbanion (k_{add}[**1**], Scheme 2) is much faster than protonation of the intermediate by the solvent water and buffer catalysts ($k_{-p} = k_{HOH} + k_{BH}$[BH]). This allows the determination of rate constants for deprotonation of **2** as the observed first-order rate constants for Claisen addition of **1** ([**1**]$_o$ = 10 mM]. We report here the observed rate constants for deprotonation of **2** between pH 2 and 7 in the presence of several buffer catalysts. These data provide a thorough description of the kinetic acidity of the different ionic forms of **2** and estimates of the effect of the protonation of basic sites of the pyridoxal cofactor on carbon acid pK_a. This analysis of the effect of formation of a covalent adduct between **1** and glycine on the kinetic acidity of the α-hydrogen of glycine is used to estimate the contribution of covalent catalysis by PLP to the rate acceleration for alanine racemase catalyzed racemization of alanine.

RESULTS

The reaction of glycine (100 mM) and **1** (10 mM) in D_2O buffered at pD 7.0 with 100 mM phosphate at 25 °C ([B]/[BD] = 1.0, I = 1.0, KCl) was monitored by ^{1}H NMR as described in the Experimental Section. The first-order *disappearance* of **1** ($k_{obsd} = 4.3 \times 10^{-5}$ s^{-1}) to form an equilibrium mixture containing 3% reactant (in the form of free aldehyde **1**, hydrated aldehyde and glycine iminium ion adduct (**2**)) and 97% of diastereomeric Claisen-type addition products (Scheme 2) in a ratio of 2:1 was observed. There was no detectable (< 1%) incorporation of deuterium from D_2O into glycine or transamination to give 5′-deoxypyridoxamine. The structures of the products of this reaction were identified as **4a** and **4b** by comparison of their NMR spectra to an authentic mixture of these compounds prepared from the reaction of **1** and aminomalonic acid.[26] Good mass balance was observed over a period of 12 hours. This shows that Claisen-type addition of glycine with **1** is the only significant reaction during this time.[25] The reaction of **1** (10 mM) and glycine (100 mM) in H_2O at pH 6.5 under the same conditions (100 mM phosphate, ([B]/[BD] = 1.0, I = 1.0, KCl) was monitored at 412 nm. This reaction was also first order for four reaction halftimes ($k_{obsd} = 5.0 \times 10^{-5}$ s^{-1}). We conclude that there is a small solvent deuterium isotope effect on the Claisen-type addition reaction when [**1**]$_o$ = 10 mM.

Figure 1 shows time courses for the reaction of glycine (100 mM) with 0.1 mM **1** in H_2O at pH 6.5 and in D_2O at pD 7.0 buffered by 100 mM phosphate ([BL]/[B] = 1.0) at 25 °C and I = 1.0 (KCl). These reactions are no longer first-order in [**1**] and no stable endpoint is observed even after 40 halftimes, using a halftime calculated for the first-order reaction of 10 mM **1** under the same conditions. These data show that there is a shift in the reaction order from first-order when [**1**]$_o$ = 10 mM towards second-order when [**1**]$_o$ is decreased 100-fold to 0.10 mM. This is consistent with the mechanism shown in Scheme 2 where: (1) Formation of the carbanion reaction intermediate by k_p is irreversible and rate determining at high [**1**] (k_{add}[**1**]

$\gg k_{-p}$) when $[\mathbf{1}]_o$ = 10 mM, and (2) Formation of the carbanion **3** becomes partly reversible, and its trapping by addition to **1** partly rate determining ($k_{add}[\mathbf{1}] \leq k_{-p}$) as the concentration of **1** is decreased 100-fold to 0.10 mM.

The initial velocity for the reaction of $[\mathbf{1}]_o$ = 0.1 mM 5′-deoxypyridoxal in D_2O is 1.8-fold *larger* than in H_2O (Figure 1). This contrasts with the 14% *smaller* value of k_{obsd} for the reaction of **1** in D_2O than in H_2O when $[\mathbf{1}]_o$ = 10 mM and the reactions are followed for 4-halftimes (see above). The smaller velocity for the reaction in H_2O compared to D_2O, when k_{add} is partly rate-determining, is due to the normal primary deuterium isotope effect on the protonation of **3** (k_p, Scheme 2) which favors return of **3** to reactant in H_2O.[27,28] Therefore, a larger fraction of the ionization steps that produce **3** in D_2O result in partitioning to the product of the Claisen-type addition reaction, and a faster reaction than in H_2O where partitioning to regenerate reactant is favored. This paper focuses on the reaction of glycine and $[\mathbf{1}]_o$ = 10 mM where deprotonation of **3** ($k_p = k_{HO}[HO] + k_B[B]$, Scheme 2) is rate determining for the formation of **4**. More extensive data for Claisen-type addition of **1** when $[\mathbf{1}]_o$ = 0.10 mM will be presented in a later paper.[29]

First-order rate constants k_{obsd} for the reaction of glycine with **1** ($[\mathbf{1}]_o$ = 10 mM) in H_2O at pH 2 - 7 and 25 °C were determined as the observed rate constant for conversion of **1** to **4** under conditions where deprotonation of **2** is rate determining for formation of **4** (Scheme 2). The reaction progress was normally monitored at 412 nm after making a 100-fold dilution using the original reaction buffer. Figure 2 shows representative plots of k_{obsd} against the concentration of acetate buffer for the Claisen-type addition reaction of **1** (10 mM) with 100 mM glycine at different fixed ratios of the buffer acid and conjugate base at I = 1.0 (KCl). Figure 3 shows plots of k_{obsd} against the concentration of phosphate buffer for the Claisen-type addition reaction of **1** (10 mM) with 100 mM glycine at different fixed ratios of the buffer acid and conjugate base at I = 1.0 (KCl). No data for the Claisen-type addition reaction is presented for reactions at pH > 7.1. As the pH is increased above 8 an additional reaction that results in addition of 2 moles of glycine to **1** to form **5** is observed. We have not fully characterized this second reaction.[30]

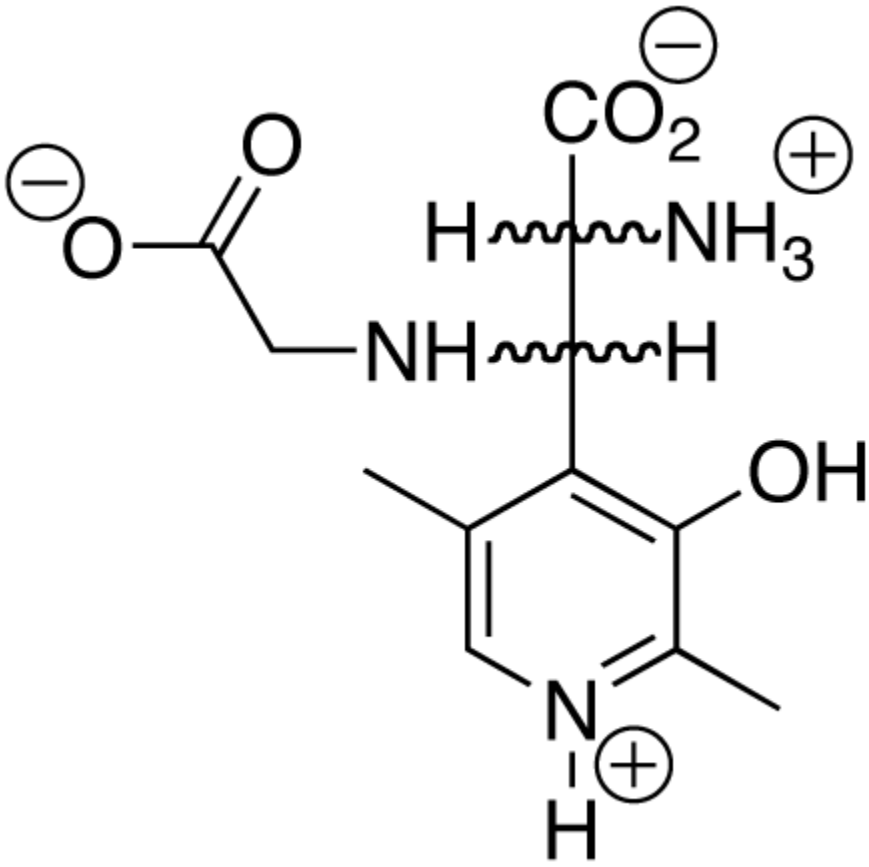

5

The *y*-intercepts of the plots shown in Figures 2 and 3, ($(k_o)_{obsd}$, s^{-1}) are reported in Table 1. Table 1 also reports values of f_{Im}, the fraction of total **1** present as the reactive iminium ion **2** under the given experimental reaction conditions. Combining f_{Im} with the observed rate constants for the Claisen-type reaction of **1** gives the first-order rate constants for buffer-independent deprotonation of **2** [$(k_0)_{Im} = (k_0)_{obsd}/f_{Im}$, Table 1].

Figure 4 shows plots of k_{obsd} against the concentration of the basic form of chloroacetate buffer (50% free base) for the Claisen-type addition reaction of **1** (10 mM) with different fixed concentrations of glycine at 25 °C and I = 1.0 (KCl). The slopes of these correlations are proportional to the concentration of glycine, because of the bimolecular reaction of glycine to form the reactive iminium ion **2** (see below). The *y*-intercept increases with the square of $[glycine]_T$ for a reaction where one molecule of glycine reacts with **1** to form **2** and the second molecule acts as a buffer catalyst of deprotonation of **2**. The inset to Figure 4 shows the plot of k_{int}/f_{Im} against the concentration of glycine zwitterion, where $k_{int} = k_o + k_B[^+H_3NCH_2CO_2^-]$ is the intercept from the main Figure, and f_{Im} is the fraction of **1** converted to **2** determined by ^1H NMR analysis (Table 1). The intercept of the plot shown in the inset, $(k_0)_{Im} = 2.3 \times 10^{-5}$ s^{-1}, is equal to the first-order rate constant for buffer- and glycine-independent deprotonation of **2** at pH 2.7 (Table 1) and the slope is the apparent second-order rate constant for deprotonation of **2** catalyzed by the basic form of glycine (see below).

Values of k_{obsd} at increasing concentrations of chloroacetate buffers (20% and 80% free base) were determined for the Claisen-type addition reaction of **1** (10 mM) with three different fixed concentrations of glycine (0.05, 0.10 and 0.20 M) at 25 °C and constant ionic strength of 1.0 (KCl). These data were evaluated as discussed for Figure 4 to give the values of $(k_0)_{Im}$ for buffer-independent deprotonation of **2** at pH 2.1 and 3.3 reported in Table 1. Table 1 shows

that deprotonation of **2** by 0.10 M glycine at pH 3.6 is slow compared with the reaction catalyzed by the stronger base acetate ion and makes only a *ca* 15% contribution to the value of $(k_{Im})_o$ at pH 3.6. This is because the general base-catalyzed reaction of 0.10 M glycine zwitterion occurs in competition with the hydroxide ion-catalyzed reaction of solvent [see Discussion]. Therefore, the largest relative rate acceleration for general-base catalysis is observed at pH < pK_a for the base catalyst, where the concentration of the Brønsted base is greatest relative to hydroxide ion; and, the importance of catalysis falls off sharply as the pH is increased above the catalyst pK_a, because now the concentration of the strong base HO^- is increasing relative to the concentration of the weak Brønsted base.[31] It is assumed, therefore, that the glycine-catalyzed reaction does not make a significant contribution to $(k_o)_{Im}$ for the deprotonation of **2** at pH > 3.6.

The slopes of the linear plots of k_{obsd} against total buffer concentration shown in Figures 2 and 3 are equal to $(k_{buf})_{obsd}$, the apparent second-order rate constants for buffer-catalyzed Claisen-type addition of glycine to **1**. Buffer catalysis is due exclusively to the basic form of the buffer (see Discussion), and the apparent rate constants for general base catalysis reported in Table 2 were calculated as $(k_B)_{obsd} = (k_{buf})_{obsd}/f_B$, where f_B is the fraction of the buffer present in the basic form. Combining $(k_B)_{obsd}$ with the fraction of **1** present as the imine (f_{Im}) gives the values for the second-order rate constants for deprotonation of **2** by the corresponding Brønsted base catalyst [$(k_B)_{Im} = (k_B)_{obsd}/f_{Im}$, Table 2]. The values of $(k_B)_{Im}$ for the reaction catalyzed by chloroacetate remain constant, within the error of these experiments (*ca* ± 10%) as the concentration of glycine is increased from 0.050 - 0.20 M. The values of $(k_B)_{Im}$ for deprotonation of **2** by glycine zwitterion reported in Table 2 were determined as the slope of k_{int}/f_{Im} against the basic form of glycine. The plot for reactions at pH 2.7 is shown in the inset to Figure 4.

DISCUSSION

Acetone is an effective catalyst of the deprotonation of glycine methyl ester in D_2O.[8] By analogy, we expected that the pyridoxal analog **1** would be an effective catalyst of deprotonation of glycine and that reversible proton transfer would lead to transfer of deuterium from solvent to the amino acid. We were surprised to observe exceedingly small levels of **1**-catalyzed exchange of the α-hydrogen of glycine after prolonged incubation in D_2O. Instead, **4a** and **4b** form as the major products of the reaction of the pyridoxal-stabilized glycine carbanion **3** (Scheme 2).[25] The decarboxylation reaction of aminomalonate catalyzed by **1** has also been reported to give **4a** and **4b** as the major products of the reaction of the pyridoxal stabilized glycine carbanion **3** generated by decarboxylation of a pyridoxal-aminomalonate adduct.[26]

Figure 1 shows that there is a 1.8-fold inverse solvent deuterium isotope effect on the initial velocity for the reaction of 0.1 mM **1** with 0.10 M glycine This provides strong evidence for the *existence* of the pyridoxal-stabilized carbanion **3** as an intermediate of the stepwise reaction shown in Scheme 2, where addition of **3** to **1** is partly rate determining for the formation of **4**. The velocity of this Claisen-type addition reaction is proportional to $k_p f_P$, where k_p is the rate constant for deprotonation of **3** and f_P is the fraction of each **3** formed that partitions forward to product. The larger velocity in D_2O compared with H_2O is due to a normal kinetic isotope effect on the protonation of **3** ($k_{-p} = k_{LOL} + k_{BH}[BL]$) which favors return of **3** to reactant in H_2O and results in a slower rate of formation of **4** for the reaction in this solvent. Large inverse solvent deuterium isotope effects have also been observed for E1cb-type elimination reactions through a carbanion intermediate that partitions between loss of leaving group to form an alkene, and protonation to regenerate substrate which is subject to a normal primary kinetic isotope effect,[27,28] and in the fragmentation of 2-(1-hydroxybenzyl)thiamine in water through a carbanion intermediate that partitions between protonation and fragementation.[32]

The kinetic data reported here for **1**-catalyzed deprotonation of glycine are in qualitative agreement with the more limited data from earlier studies by Bruice and Dixon of the racemization of alanine catalyzed by the pyridoxal analog 3-hydroxyridine-4-carboxyaldehyde.[19] We have revisited this problem for **1**-catalyzed deprotonation of glycine in order to: (1) Exploit a simple kinetic method for monitoring deprotonation of **2** to obtain an extensive body of kinetic data for formation of a pyridoxal-stabilized carbanion. (2) Draw direct comparisons between the effect of the pyridoxal-analog **1** on the carbon acidity of glycine with the effect of a variety of other substituents on this carbon acidity.[8-10,33,34] (3) Obtain the rate acceleration for a PLP-assisted enzyme-catalyzed deprotonation of amino acids using modern kinetic data.

Deprotonation of 2 by Solvent

The open squares in Figure 5 show the pH rate profile for the rate constants for solvent-catalyzed Claisen addition $(k_o)_{obsd}$ determined by monitoring the disappearance of **1** at 412 nm, and the solid circles show the rate constants for rate determining deprotonation of **2** calculated as $(k_0)_{Im} = (k_0)_{obsd}/f_{Im}$, where f_{Im} is the fraction of **1** converted to the imine **2** under the experimental reaction conditions, determined by ^{1}H NMR.

Figure 5 shows that the observed rate constants (open squares) for the solvent-catalyzed Claisen-type addition reaction at low pH decrease with increasing $[H^+]$; and, that this decrease is due mainly to a decrease in the fraction of substrate present as the reactive imine **2**. The nearly flat pH rate profile for deprotonation of **2** (solid circles) reflects the increasing reactivity of **2** due to protonation of basic sites with pK_as of 6.4, 3.0 and 2.1 (Scheme 3)[35] that compensates for the decease in $[HO^-]$. The deprotonation of **2** observed in acidic solution ($[HO^-] = 10^{-12}$ M (1 picomolar!) at pH 2] is a dramatic manifestation of the strong acidity of this carbon acid.

The dominant pathway for the reaction of **2** at pH 7 is deprotonation of **2-H$_2$** by hydroxide ion. The observed rate constant is nearly pH independent because the effect of decreasing $[HO^-]$ and of increasing [**2-H$_2$**] on the reaction rate cancel. There is a downward break in the pH rate profile at pH = pK_a = 6.4 for **2-H$_2$**[35] and then an upward break at pH 5 due to a new pathway for deprotonation of **2-H$_3$** by hydroxide ion. The kinetically equivalent pathway for deprotonation of **2-H$_2$** by water is excluded, because deprotonation of amino-acids and their derivatives by water has been shown to be slow compared to the hydroxide ion-catalyzed reaction at pH 5.[9]

The second upward break in the pH rate profile at pH 4 may be due to one of two kinetically equivalent pathways; deprotonation of **2-H$_3$** (pK_a = 3.0)[35] by water, or deprotonation of **2-H$_4$** by hydroxide ion. The following observations are inconsistent with water-catalyzed deprotonation of **2-H$_3$** and provide strong evidence that the reaction at low pH is due to deprotonation of **2-H$_4$** by hydroxide ion.

1. If the reaction at low pH were water-catalyzed deprotonation of **2-H$_3$** then an upward break should be observed in the pH rate profile as **2-H$_4$** (pK_a = 2.1) accumulates at pH 2 because protonation of the carboxylate group of **2-H$_3$** should increase the reactivity of this carbon acid toward deprotonation by water. However, no upward break is observed in the pH rate profile.
2. The addition of a fixed concentration of glycine zwitterion should cause the same increase in the velocity of deprotonation of **2-H$_3$** relative to the rate of a water catalyzed reaction as the pH is decreased from 3 to 2.[31] In fact, there is a significant increase in the rate acceleration for catalysis by glycine zwitterion over this pH range (Table 1). This shows that solvent is becoming less reactive relative to the buffer as

the pH decreases and is consistent with the reaction of the conjugate base of solvent, hydroxide ion, in deprotonation of **2-H$_4$**.

$$(k_o)_{Im}=\frac{\left[(k_{HO})_{2-H4}[H^+]^2+(k_{HO})_{2-H3}(K_a)_4[H^+]+(k_{HO})_{2-H2}(K_a)_3(K_a)_4\right]K_w}{[H^+]^3+(K_a)_4[H^+]^2+(K_a)_3(K_a)_4[H^+]+(K_a)_2(K_a)_3(K_a)_4} \quad (1)$$

$$(k_o)_{Im}=\frac{(k_{HO})_{2-H2}K_w}{(K_a)_2+[H^+]} \quad (2)$$

$$(k_o)_{Im}=\frac{(k_{HO})_{2-H4}K_w[H^+]}{(K_a)_4(K_a)_3+(K_a)_4+[H^+]^2} \quad (3)$$

Equation 1 gives the relationship between the kinetic parameter $(k_o)_{Im}$ and the rate constants and acidity constants for Scheme 3.[35] The values of the second-order rate constants for deprotonation of **2-H$_2$**, **2-H$_3$**, and **2-H$_4$** by hydroxide ion were evaluated as follows for the data shown in Figure 5. (1) The only significant reaction at high pH is deprotonation of **2-H$_2$** by hydroxide ion. The value for $(k_{HO})_{\mathbf{2\text{-}H2}}$ was determined by fitting the data from Figure 5 at high pH to the limiting eq 2 which can be derived for Scheme 3 for the case where [**2-H$_3$**] = [**2-H$_4$**] = 0. (2) The only significant term at low pH is $(k_{HO})_{\mathbf{2\text{-}H4}}$ for deprotonation of **2-H$_4$**. The value of $(k_{HO})_{\mathbf{2\text{-}H4}}$ was determined by fitting the data at low pH to equation 3, which can be derived for Scheme 3 for the case where [**2-H$_2$**] = 0. (2) The deprotonation of **2-H$_3$** by hydroxide ion is the dominant reaction at intermediate pH. The value for $(k_{HO})_{\mathbf{2\text{-}H3}}$ for this reaction was determined by fitting the data at intermediate pH to eq 1 and using the values of $(k_{HO})_{\mathbf{2\text{-}H4}}$ and $(k_{HO})_{\mathbf{2\text{-}H2}}$ determined at the pH extremes, so that $(k_{HO})_{\mathbf{2\text{-}H3}}$ is the only variable in this fitting procedure. The solid line in Figure 5 shows the theoretical fit of the experimental data obtained using the acidity constants from Scheme 3 and the second-order rate constants for the hydroxide ion-catalyzed reaction determined by the above fitting procedure (Table 3).

Deprotonation of 2 by General Brønsted Bases

Buffer catalysis of the Claisen-type addition reaction is due to general base-catalyzed deprotonation of **2** to form the pyridoxal stabilized glycine carbanion **3**. There are several moderately basic sites at **2** where protonation by buffer acids will cause an increase in the reactivity of the α-imine carbon towards deprotonation. However, concerted general-acid catalysis of proton transfer is effectively prohibited by the *libido* rule of Jencks, because under our experimental reaction conditions proton transfer from the catalyst to the *reacting* form of the substrate is either thermodynamically favorable or only slightly uphill.[36] The *libido* rule states that general acid catalysis will only be observed for reactions when there is a large change in basicity of a reacting group that causes *unfavorable* protonation of the reactant by the acid catalyst to become favorable for protonation of product.[31,36]

$$(k_B)_{Im}=\frac{\left[(k_B)_{2-H4}[H^+]^3+(k_B)_{2-H3}(K_a)_4[H^+]^2+(k_B)_{2-H2}(K_a)_3(K_a)_4[H^+]\right]}{[H^+]^3+(K_a)_4[H^+]^2+(K_a)_3(K_a)_4[H^+]+(K_a)_2(K_a)_3(K_a)_4} \quad (4)$$

Figure 6 shows the pH rate profiles for the observed second-order rate constants for general base-catalyzed deprotonation of **2** $(k_B)_{Im}$. The increase in $(k_B)_{Im}$ with increasing pH is due to the increasing acidity of the substrate that results from protonation of sites at **2** with pK_as of

6.4, 3.0 and 2.1.[35] Equation 4 derived for Scheme 3 shows the relationship between $(k_B)_{Im}$ and the rate and the acidity constants for Scheme 3, where each term in this equation corresponds to the rate constant for deprotonation of a single ionic form of **2**. It was only possible to study catalysis by any single buffer over a range of 2 pH units, where only two of the three ionic forms of **2** are reacting. The solid lines in Figure 6 show the fits of the data to truncated forms of eq 2 (not shown) that were derived for Schemes that include only two of the three kinetic terms for Scheme 3 and three of the four forms of **2**. The acidity constant $(K_a)_2$ and **2H$_2$** were omitted in deriving the equation for a modified form of Scheme 3 that was used to fit the data for the catalysis by glycine and chloroacetate ions, while $(K_a)_4$ and **2H$_4$** were omitted in deriving the equation that was used to fit data for catalysis by acetate and phosphate ions. Table 3 reports the values of $(k_B)_{\mathbf{2\text{-}H4}}$, $(k_B)_{\mathbf{2\text{-}H3}}$, and $(k_B)_{\mathbf{2\text{-}H2}}$ obtained from these fits.

The slope of the Brønsted correlation (not shown) for general base catalysis of deprotonation of **2-H$_3$** is $\beta = 0.83$. Brønsted coefficients of close to 1 were observed in studies of general base catalysis of deprotonation of the cationic carbon acids of glycine and betaine methyl ester.[9] The smaller value of $\beta = 0.83$ observed here reflects a relatively small Hammond type shift to an earlier transition state caused by the greater carbon acidity of **2-H$_3$** compared to the simpler amino acid derivatives.[37]

Substituent Effects on the Acidity of Glycine

The solid symbols in Figure 7 show the rate-equilibrium relationship between second-order rate constants for deprotonation of *cationic* carbon acids by hydroxide ion and the estimated carbon acid pK_as for simple derivatives of glycine and of a related cationic carbon acid.[9] These data define a linear correlation of slope of 0.44 (Brønsted β for proton transfer) and intercept of 10.0. The carbon acid pK_as for **2-H$_4$**, **2-H$_3$** and **2-H$_2$** reported in Chart 1 were calculated by making the assumption that values of $\log(k_{OH}/2)$ from Table 3 lie on the linear correlation established for related carbon acids (open circles, Figure 7). By comparison, values of 9, 12 and 14 were estimated for the α-imino carbon acid pK_a of the corresponding protonated forms of the adduct between alanine and 3-hydroxypyridine-4-carboxaldehyde by extrapolation of linear logarithmic relationship of rate constants k_{OH} for a highly structurally diverse set of *neutral* carbon acids.[19]

Several effects contribute to the differences in the carbon acidity of **2-H$_2$**, **2-H$_3$**, and **2-H$_4$**. (1) The presumably strong intramolecular hydrogen bond between the iminium ion nitrogen and phenoxide anion of **2-H$_2$** has the effect of decreasing the carbon acidity of **2-H$_2$**, because α-carbon deprotonation reduces the acidity of the nitrogen hydrogen bond donor which weakens the hydrogen bond at the product enolate.[38] (2) Destabilizing intramolecular electrostatic interactions between cationic centers will increase the acidity of **2-H$_4$**, because these interactions are relieved at the product enolate.[39] (3) Protonation of the phenolate ion of **2-H$_2$** to form **2-H$_3$** will cause an increase in carbon acidity by increasing the charge density at nitrogen that interacts a neighboring enolate dianion.[8,9] The effect of cationic α-substituents on the stability of enolates is known to be particularly large.[9,40,41] (4) Finally, neutralization of charge at a carboxylate anion will cause an increase in the acidity of neighboring carbon by allowing the formation of an unstable enolate dianion to be avoided.[42,43] For example, there is an 8 unit difference in the pK_as for deprotonation of the α-amino carbon of glycine zwitterion (pK_a = 29) and N-protonated glycine methyl ester (pK_a = 21).[9]

The pK_a of 6 for carbon deprotonation of **2-H$_4$** is striking in comparison to the carbon-acid pK_a of *ca* 34 for glycine carboxylate anion.[44] A large portion of the reduction in carbon acid pK_a can be obtained with relatively simple modifications of the carboxylate oxygen and amino nitrogen of glycine. For example a pK_a of 14 was estimated for deprotonation of the α-imino carbon of the iminium ion adduct between acetone and glycine methyl ester.[8] The *ca* 8-unit

lower pK_a estimated for the α-imino carbon of **2-H$_4$** reflects specific stabilization of charge by the elaborate electron sink of the pyridoxal cofactor. It is not possible to generate a significant concentration of this "quininoid"-type carbanion by deprotonation of **2-H$_4$**, because **2-H$_4$** only accumulates at a pH 3 that is below the pK_a for the carbon acid. Our data suggest that it should be possible to generate a "quininoid"-type carbanion by deprotonation of an analog of **2-H$_4$** where protons at the imine nitrogen and carboxylic acid are replaced by alkyl groups.[45]

Enzymatic Catalysis

The PLP analog of **2-H$_4$** is the most acidic form of the cofactor, and the fully protonated cofactor might be expected to be the species selected to undergo enzyme-catalyzed deprotonation at the α-imino acid carbon. However, X-ray crystal structures of pyridoxal enzymes show the cofactor bound in the form analogous to **2-H$_2$**,[46-48] or in the case of alanine racemase the form analogous to **2H**.[49] This is evidence that despite the weak carbon acidity of **2H$_2$** (p$K_a \approx 17$) and even weaker acidity of **2-H**, these forms of the cofactor are selected for deprotonation by enzyme catalysts. There are several reasons why these enzyme-catalyzed reactions are unlikely to proceed by deprotonation of **2-H$_4$**. (1) The equilibrium constant for formation of **2-H$_4$** from glycine and **1** is less favorable than for formation of **2-H$_3$** and **2-H$_2$** (Table 1). (2) There is a substantial thermodynamic barrier to formation of **2-H$_4$** from **2-H**, the most abundant form of the cofactor at pH 7. (3) There are minimal ionic groups at **2-H$_4$** to interact with groups of opposing charge at the enzyme active site. Note that the intramolecular hydrogen bond between nitrogen and oxygen at **2-H$_2$** will reduce its carbon acidity (see above). However, the carbon acidity will be increased if **2-H$_2$** is bound in a conformation where the intramolecular hydrogen bond cleaved. The energetic price for cleavage of the hydrogen bond may be recovered as stabilizing interactions between the protein and the charged nitrogen and oxygen.

A value of $(k_B)_{\mathbf{2\text{-}H2}} = 1.7\times10^{-3}$ M^{-1} s^{-1} (Table 3) was determined for deprotonation of **2-H$_2$** by phosphate dianion (pK_a = 6.5), a reaction where the base catalyst and carbon acid combine to form a transition state for deprotonation of the α-imino carbon. By comparison $k_{cat}/K_m = 4 \times 10^5$ M^{-1} s^{-1} for alanine racemase (*Bacillus stearothermophilus*) catalyzed racemization of D-alanine at 25 °C, a reaction where the enzyme and alanine combine to form a *virtual* transition state for deprotonation of the α-imino carbon of an alanine-PLP adduct.[50] A comparison of these second-order rate constants shows that the presence of the protein catalysts causes a 2×10^8-fold rate increase in the apparent second-order rate constant for proton transfer. This is close to the true rate acceleration for carbon-acid deprotonation, which is mostly rate determining for the alanine racemase catalyzed reaction.[23,50,51] This corresponds to a *ca* 11 kcal/mol stabilization of the transition state for deprotonation of the α-imino carbon.[52] A much larger 19 kcal/mole transition state stabilization was estimated for non-PLP amino acid racemases,[5] so that the cofactor bears about one-half the burden of catalysis of the proton transfer reaction.

A smaller transition state stabilization of 8 kcal/mole has been estimated in a combined QM/MM computational study of the solution and enzyme catalyzed reaction.[24] The difference in the results of the experimental and computational studies is due in part to our choice of phosphate dianion as the base that abstracts a proton from the amino acid substrate. By comparison a more basic phenoxide anion was used in computational studies to model the phenoxide anion of tyrosine which is thought to serve as the base in the alanine racemase catalyzed reaction.[50,53,54] The correct choice of the solution base to model an active site side-chain whose pK_a has not been rigorously determined is problematic. We therefore consider the results of experiments and calculations to have converged to give a single consistent picture of the energetics for the solution and enzyme-catalyzed reactions.

EXPERIMENTAL

General

Pyridoxal 5′-phosphate, glycine, K_2HPO_4, KH_2PO_4, potassium acetate, glacial acetic acid, and potassium chloride were purchased from Fluka. 5′-Deoxypyridoxal was prepared by published procedures from pyridoxal 5′-phosphate.[55] Reagent grade inorganic chemicals were used without further purification. The water used for kinetic experiments was first distilled and then passed through a Milli-Q water purification system.

Preparation of solutions

The solution pH was determined at 25 °C using an Orion model 720A pH meter equipped a Radiometer pH4006-9 combination electrode. The pH of solutions of glycine was adjusted to the pH desired for the kinetic experiment, a concentrated solution of KCl was added and the volume adjusted with distilled water to give the desired final concentration of glycine at I = 1.0 (KCl). Phosphate and acetate buffers were prepared at I = 1.0 (KCl) by mixing measured volumes of stock solutions of the buffer acid and conjugate base. Chloroacetate buffers were prepared at I = 1.0 (KCl) by addition of a measured volume of 1.00 M KOH to a solution of chloroacetic acid.

The diastereomers of the Claisen adduct between glycine and **1** (Scheme 2) were prepared by following a published procedure.[26] ^{1}H NMR (D_2O, pD 7.0, chemical shifts reported relative to HOD at 4.67 ppm): Major diastereoisomer: δ 2.24, 2.40 (3H, s, CH_3), 3.95 (1H, d, J = 5 Hz, $CH(ND_3)^+$), 5.29 (1H, d, J = 5 Hz, CH(OD)), 7.45 (1H, s, ArH); Minor diastereoisomer: δ 2.29, 2.37 (3H, s, CH_3), 4.21 (1H, d, J = 5 Hz, $CH(ND_3)^+$), 5.50 (1H, d, J = 5 Hz, CH(OD)), 7.41 (1H, s, 1H, ArH). Anal. ($C_{10}H_{16}Cl_2N_2O_4$) C, H, N.

^{1}H NMR spectroscopy

^{1}H NMR spectra were recorded on a Varian Unity Inova-500 spectrometer. ^{1}H NMR spectra in D_2O were obtained as described in earlier work.[9,56] ^{1}H NMR spectra in neat H_2O were obtained with suppression of the peak for HOH and by using DOD in an inner tube for shimming the spectrometer. Chemical shifts were referenced to HOD at 4.67 ppm. In all cases a sweep width of 6000 Hz, a 90° pulse angle, and an acquisition time of 6 s was employed. The relaxation delay between pulses was at least 7-fold longer than the longest T_1 of the protons under examination. Baselines were subjected to first-order drift correction before integration of the signals.

The fraction of **1** present as the iminium ion in H_2O under the conditions of the kinetic experiments was determined by ^{1}H NMR analyses. A solution of 0.5 M **1** in CD_3CN was injected into water that contains 0.10 M of the appropriate buffer, 0.1 M glycine and 1 mM of the internal standard tetramethylammonium hydrogen sulfate to give a final concentration of 10 mM **1** at I = 1.0 (KCl). ^{1}H NMR spectra were recorded at 25 °C approximately 1 hour after the addition of **1**. The fraction of **1** present as the glycine iminium ion was determined from the normalized peak areas of a single proton for **1**, the hydrate of **1** and the iminium ion **2**.

Kinetic analyses by ^{1}H NMR spectroscopy

The reaction of **1** with glycine to form the Claisen-type adduct was followed by monitoring the disappearance of reactant by ^{1}H NMR in H_2O or D_2O. Solutions of 10 mM **1** were prepared by making a 50-fold dilution of a 0.50 M solution of **1** in CD_3CN into water that contains 0.10 M buffer, 0.10 M glycine and 1 mM of the internal standard tetramethylammonium hydrogen sulfate at I = 1.0 (KCl). The ^{1}H NMR spectra were recorded at 25 °C. The first spectrum was obtained *ca* one hour after the addition of **1**. The relative concentrations of **1**, **1**-hydrate and the **2** were determined from relative normalized peak areas, $(A)_{nor}$ for each compound. The

sum of these areas, ΣA_N, was determined using the peak areas for the protons (N) whose signals were resolved. The signals for the nonexchangable protons of the different forms of the cofactor were often all resolved, in which case N = 8. However, the chemical shifts are pH dependent and at some pH it was not possible to resolve the signals for all of the protons. In these cases N is equal to the number of protons that gave cleanly resolved signals. First-order rate constants for the reactions of **1** were determined as the slope of semilogarithmic plots of reaction progress against time (eq 5), where $(\Sigma\text{-}A_N)_t$ and $(\Sigma\text{-}A_N)_\infty$ are the sum of the areas for the signals for the cleanly resolved protons at reaction time *t* and after ten reaction halftimes, respectively. These plots were linear for four reaction halftimes

$$(\Sigma A_N)_t = \left[(\Sigma A_N)_t - (\Sigma A_N)_\infty \right] \quad (5)$$

Kinetic analyses by UV-Vis spectroscopy

The reaction of **1** with glycine to form **4** (Scheme 2) was followed by monitoring the decrease in absorbance at 412 nm for reactions at 25 °C. The reactions were initiated by diluting a 0.50 M solution of **1** in acetonitrile into aqueous buffered solutions to give a final concentration of 10 mM **1** at I = 1.0 (KCl). For reactions at pH > 2.7 the absorbance at 412 of 10 mM **1** was too large to determine by direct measurement. Therefore, the absorbance at measured reaction times was determined immediately after making a 100-fold dilution of an aliquot from the reaction mixture into a solution of the same composition. Pseudo first-order rate constants k_{obsd} (s^{-1}) for Claisen-type addition of glycine to **1** ($[\mathbf{1}]_o$ = 10 mM) were determined as the slope of semilogarithmic plots of reaction progress against time, which were linear for at least three reaction halftimes. The rate constants were reproducible to ± 5%.

The slow Claisen-type addition reactions at pH ≤ 2.7 were monitored by directly following the decrease in absorbance at 412 nm. The endpoints were determined as the absorbance of a 10 mM solution of the chemically synthesized Claisen adduct reaction product. First-order rate constants k_{obsd} (s^{-1}) were determined by the method of initial rates as the slopes of linear plots of reaction progress against time for the first 10% of the reaction. Observed second-order rate constants (k_B, M^{-1} s^{-1}) for buffer-catalyzed Claisen-type addition of glycine to **1** were determined as the slopes of linear plots of k_{obsd} against the concentration of the basic form of the buffer.

Acknowledgment

We acknowledge National Institutes of Health Grant GM 39754 for generous support of this work.

REFERENCES

(1). Puig E, Garcia-Viloca M, Gonzalez-Lafont A, Lluch JM. J. Phys. Chem. A 2006;110:717–725. [PubMed: 16405345]

(2). Pillai B, Cherney MM, Diaper CM, Sutherland A, Blanchard JS, Vederas JC, James MNG. Proc. Nat. Acad. Sci. (USA) 2006;103:8668–8673. [PubMed: 16723397]

(3). Buschiazzo A, Goytia M, Schaeffer F, Degrave W, Shepard W, Gregoire C, Chamond N, Cosson A, Berneman A, Coatnoan N, Alzari PM, Minoprio P. Proc. Nat. Acad. Sci. (USA) 2006;103:1705–1710. [PubMed: 16446443]

(4). Richard JP, Amyes TL. Biorg. Chem 2004;32:354–366.

(5). Williams G, Maziarz EP, Amyes TL, Wood TD, Richard JP. Biochemistry 2003;42:8354–8361. [PubMed: 12846584]

(6). Martell AE. Adv. Enz. Rel. Areas. Mol. Biol 1982;53:163–199.

(7). Adams E. Adv. Enz. Rel. Areas. Mol. Biol 1976;44:69–138.

(8). Rios A, Crugeiras J, Amyes TL, Richard JP. J. Am. Chem. Soc 2001;123:7949–7950. [PubMed: 11493086]
(9). Rios A, Amyes TL, Richard JP. J. Am. Chem. Soc 2000;122:9373–9385.
(10). Rios A, Richard JP, Amyes TL. J. Am. Chem. Soc 2002;124:8251–8259. [PubMed: 12105903]
(11). Eliot AC, Kirsch JF. Ann. Rev. Biochem 2004;73:383–415. [PubMed: 15189147]
(12). Toney MD, Kirsch JF. Biochemistry 1993;32:1471–1479. [PubMed: 8431426]
(13). Snell EE. Coenzymes and Cofactors 1986;1:1–12.
(14). Snell EE, Di Mari SJ. Enzymes (3rd Ed.) 1970;2:335–370.
(15). Toney MD. Arch. Biochem. Biophys 2005;433:279–287. [PubMed: 15581583]
(16). Christen P, Mehta PK. Chem. Rec 2001;1:436–447. [PubMed: 11933250]
(17). Auld DS, Bruice TC. J. Am. Chem. Soc 1967;89:2098–2106.
(18). Auld DS, Bruice TC. J. Am. Chem. Soc 1967;89:2090–2097.
(19). Dixon JE, Bruice TC. Biochemistry 1973;12:4762–4766. [PubMed: 4773854]
(20). Chruma JJ, Liu L, Zhou W, Breslow R. Bioorg. Med. Chem. Lett 2005;13:5873–5883.
(21). Koh JT, Delaude L, Breslow R. J. Am. Chem. Soc 1994;116:11234–11240.
(22). Weiner W, Winkler J, Zimmerman SC, Czarnik AW, Breslow R. J. Am. Chem. Soc 1985;107:4093–4094.
(23). Spies MA, Woodward JJ, Watnik MR, Toney MD. J. Am. Chem. Soc 2004;126:7464–7475. [PubMed: 15198593]
(24). Major DT, Nam K, Gao J. J. Am. Chem. Soc 2006;128:8114–8115. [PubMed: 16787057]
(25). Toth K, Amyes TL, Richard JP, Malthouse JPG, NíBeilliu ME. J. Am. Chem. Soc 2004;126:10538–10539. [PubMed: 15327301]
(26). Thanassi JW. Biochemistry 1970;9:525–532. [PubMed: 5415959]
(27). Keeffe JR, Jencks WP. J. Am. Chem. Soc 1983;105:265–279.
(28). Keeffe JR, Jencks WP. J. Am. Chem. Soc 1981;103:2457–2459.
(29). Richard, John P.; Toth, Krysztina. in preparation for publication
(30). Toth K, Gaskell LM, Richard JP. J. Org. Chem 2006;71:7094–7096. [PubMed: 16930073]
(31). Jencks WP. Acc. Chem. Res 1976;9:425–432.
(32). Ikeda G, Kluger R. J. Phys. Org. Chem 2004;17:507–510.
(33). Rios A, Richard JP. J. Am. Chem. Soc 1997;119:8375–8376.
(34). Crugeiras J, Rios A, Amyes TL, Richard JP. Org. & Biomol. Chem 2005;3:2145–2149. [PubMed: 15917903]
(35). Vazquez MA, Echevarria G, Munoz F, Donoso J, Garcia Blanco F. J. Chem. Soc., Perkins Trans. 2 1989:1617–1622.
(36). Jencks WP. J. Am. Chem. Soc 1972;94:4731–4732.
(37). Hammond GS. J. Am. Chem. Soc 1955;77:334–338.
(38). Stahl N, Jencks WP. J. Am. Chem. Soc 1986;108:4196–4205.
(39). Hine, J. Structural Effects on Equilibria in Organic Chemistry. Wiley; New York: 1975. p. 98
(40). Tobin JB, Frey PA. J. Am. Chem. Soc 1996;118:12253–12260.
(41). Halkides CJ, Frey PA, Tobin JB. J. Am. Chem. Soc 1993;115:3332–3333.
(42). Richard JP, Williams G, O'Donoghue AC, Amyes TL. J. Am. Chem. Soc 2002;124:2957–2968. [PubMed: 11902887]
(43). Gao J. Theochem 1996;370:203–208.
(44). The carbon acid pKa for glycine anion should be greater than the value of 33.5 reported for acetate anion [ref [40]].
(45). Metzler CM, Harris AG, Metzler DE. Biochemistry 1988;27:4923–4933. [PubMed: 3167020]
(46). Toney MD, Hohenester E, Cowan SW, Jansonius JN. Science 1993;261:756–759. [PubMed: 8342040]
(47). Kirsch JF, Eichele G, Ford GC, Vincent MG, Jansonius JN. J. Mol. Biol 1984;174:497–525. [PubMed: 6143829]

(48). Almo SL, Smith DL, Danishefsky AT, Ringe D. Prot. Eng 1994;7:405–412.
(49). Shaw JP, Petsko GA, Ringe D. Biochemistry 1997;36:1329–1342. [PubMed: 9063881]
(50). Sun S, Toney MD. Biochemistry 1999;38:4058–4065. [PubMed: 10194319]
(51). Spies MA, Toney MD. Biochemistry 2003;42:5099–5107. [PubMed: 12718553]
(52). Richard JP. J. Am. Chem. Soc 1984;106:4926–4936.
(53). Watanabe A, Kurokawa Y, Yoshimura T, Esaki N. J. Biochem 1999;125:987–990. [PubMed: 10348897]
(54). Watanabe A, Yoshimura T, Mikami B, Esaki N. J. Biochem 1999;126:781–786. [PubMed: 10502689]
(55). Cunningham WC, Thanassi JW. Experimentia 1979;35:451–452.
(56). Amyes TL, Richard JP. J. Am. Chem. Soc 1996;118:3129–3141.

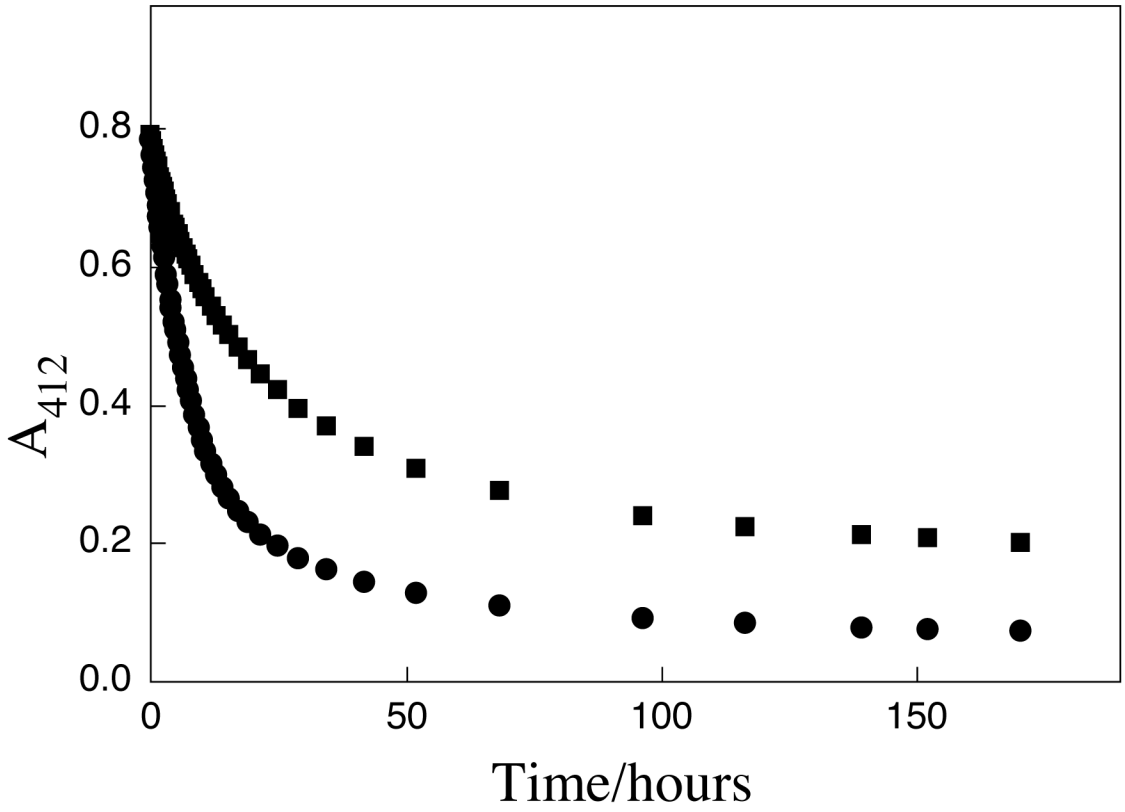

Figure 1.
Time courses for reaction of glycine (100 mM) with 0.1 mM **1** in H_2O at pH 6.5 (■) and in D_2O (●) at pD 7.0 buffered by 100 mM phosphate ([BL]/[B] = 1.0) at 25 °C and *I* = 1.0 (KCl).

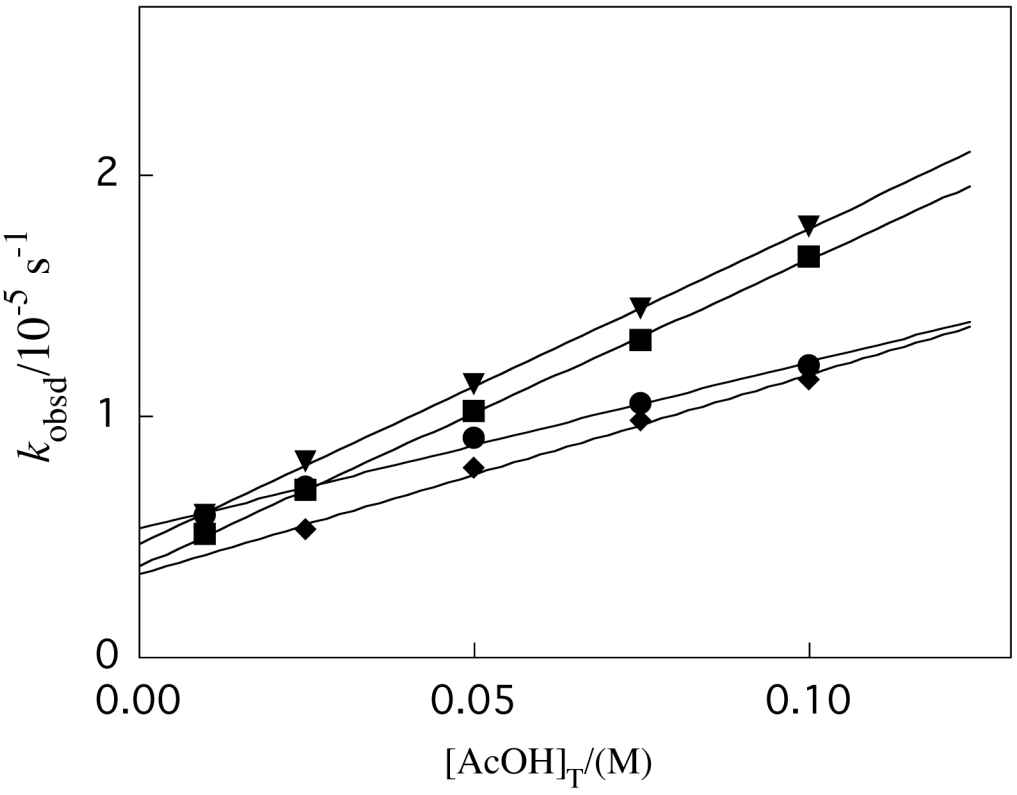

Figure 2.

The effect of increasing concentrations of acetate buffer on k_{obsd} for Claisen-type addition of glycine (100 mM) to **1** (10 mM) at constant ionic strength of 1.0 (KCl) and 25 °C. Key: (◆), [AcO^-]/[AcOH] = 4.0; (■), [AcO^-]/[AcOH] = 1.0; (▼), [AcO^-]/[AcOH] = 0.25; (●), [AcO^-]/[AcOH] = 0.10

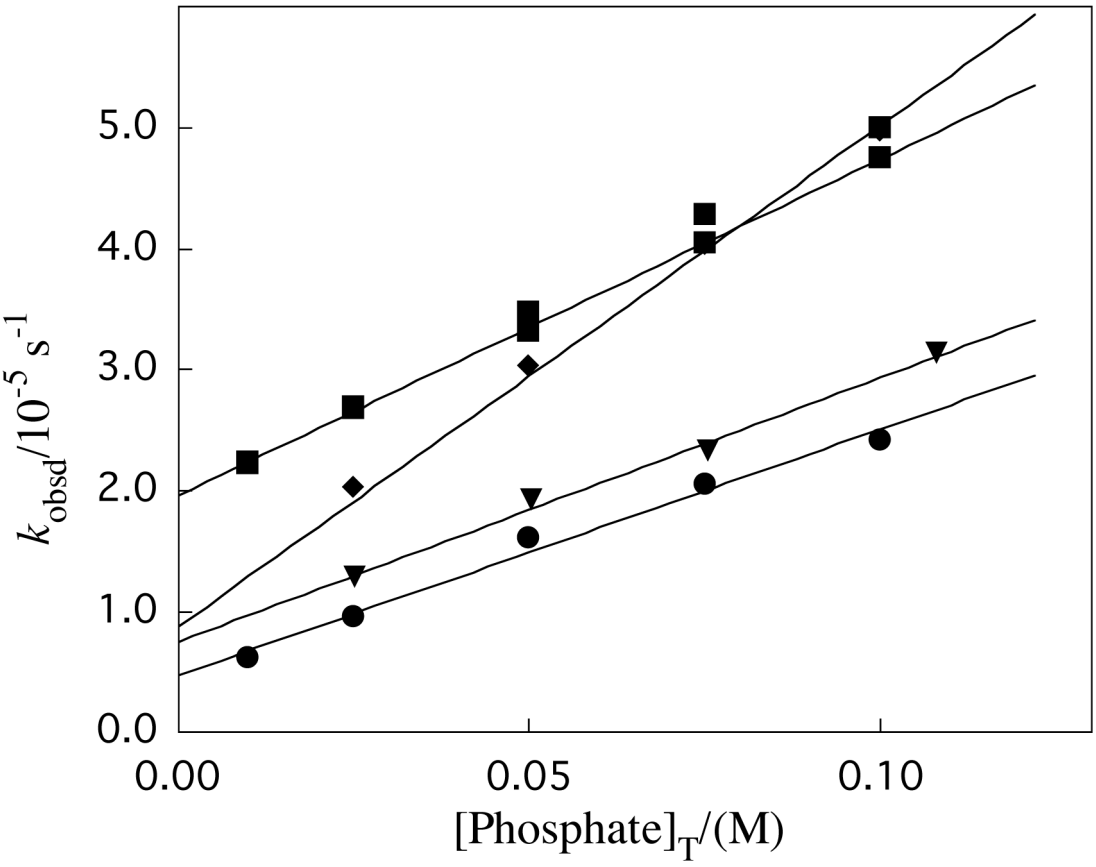

Figure 3.

The effect of increasing concentrations of phosphate buffer on k_{obsd} for Claisen-type addition of glycine (100 mM) to **1** (10 mM) at constant ionic strength of 1.0 (KCl) and 25 °C. Key: (■), $[HPO_4^{2-}]/[H_2PO_4^-]$ = 4.0; (◆), $[HPO_4^{2-}]/[H_2PO_4^-]$ = 1.0; (▼), $[HPO_4^{2-}]/[H_2PO_4^-]$ = 0.25; (●), $[HPO_4^{2-}]/[H_2PO_4^-]$ = 0.10

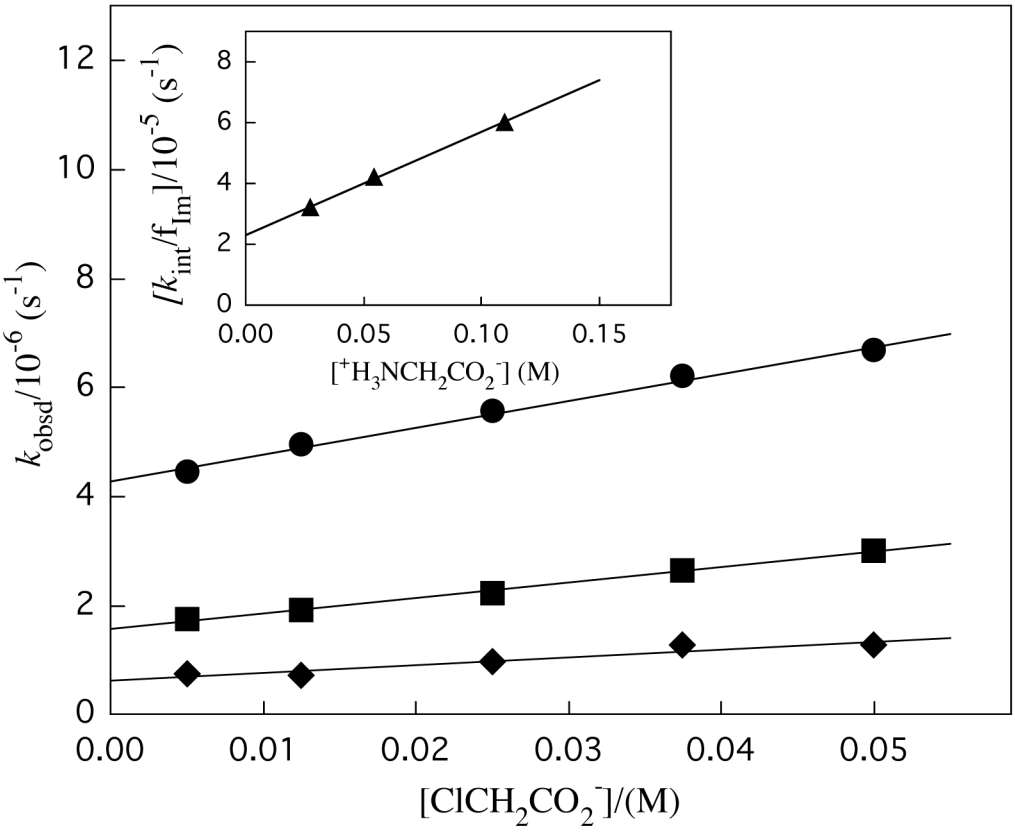

Figure 4.
The effect of increasing concentrations of the basic form of chloroacetate buffer (50% free base) on k_{obsd} for Claisen-type addition of glycine to **1** (10 mM) at increasing fixed concentrations of glycine and constant ionic strength of 1.0 (KCl) at 25 °C. Key: (◆), 0.05 M glycine; (■), 0.10 M glycine; (●), 0.20 M glycine.

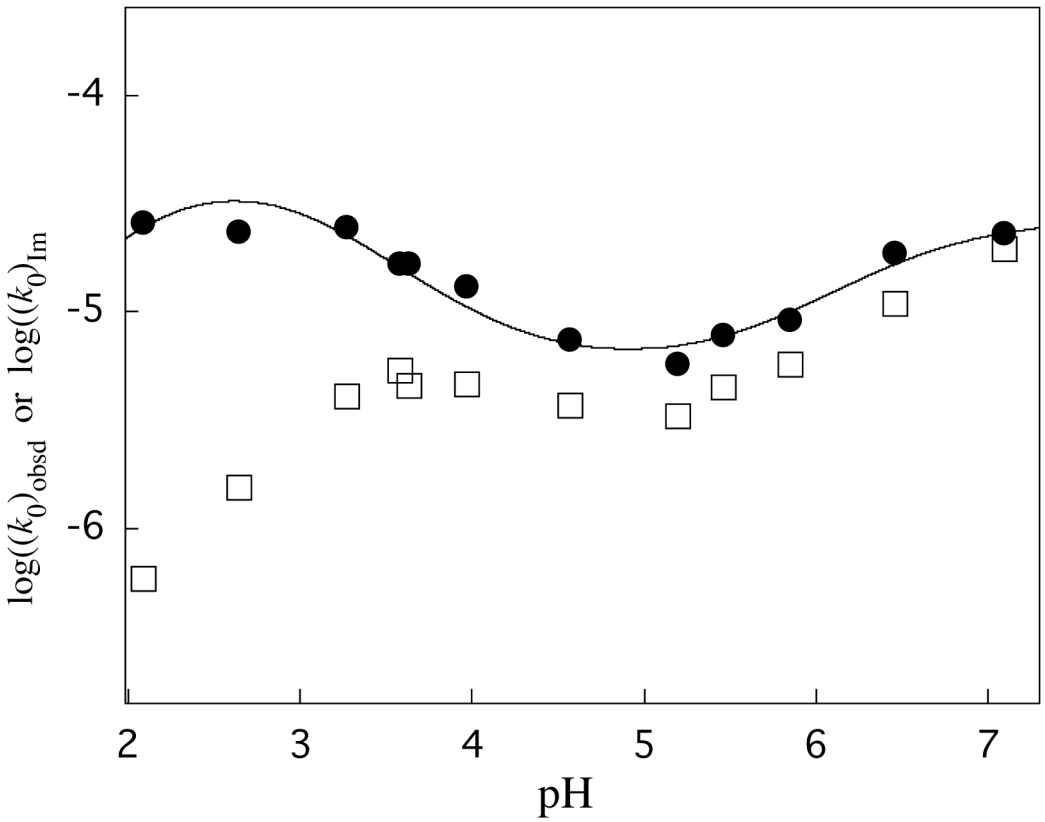

Figure 5.

pH rate profiles for the observed rate constants for the solvent-catalyzed Claisen-type addition reaction between glycine and **1** ($(k_o)_{obsd}$ (s^{-1}), □), and the derived rate constants for Scheme 2 where deprotonation of **2** is the rate determining step for Claisen-type addition (**(**$(k_o)_{Im}$ (s^{-1}), ●) for reactions at 25 °C and I = 1.0 maintained with KCl (Table 1). The solid line shows the least squares fit of the data to eq 1 using the acidity constants from Scheme 3,[35] and the derived second-order rate constants for deprotonation of **2-H$_4$, 2-H$_3$**, and **2-H$_2$** by hydroxide ion.

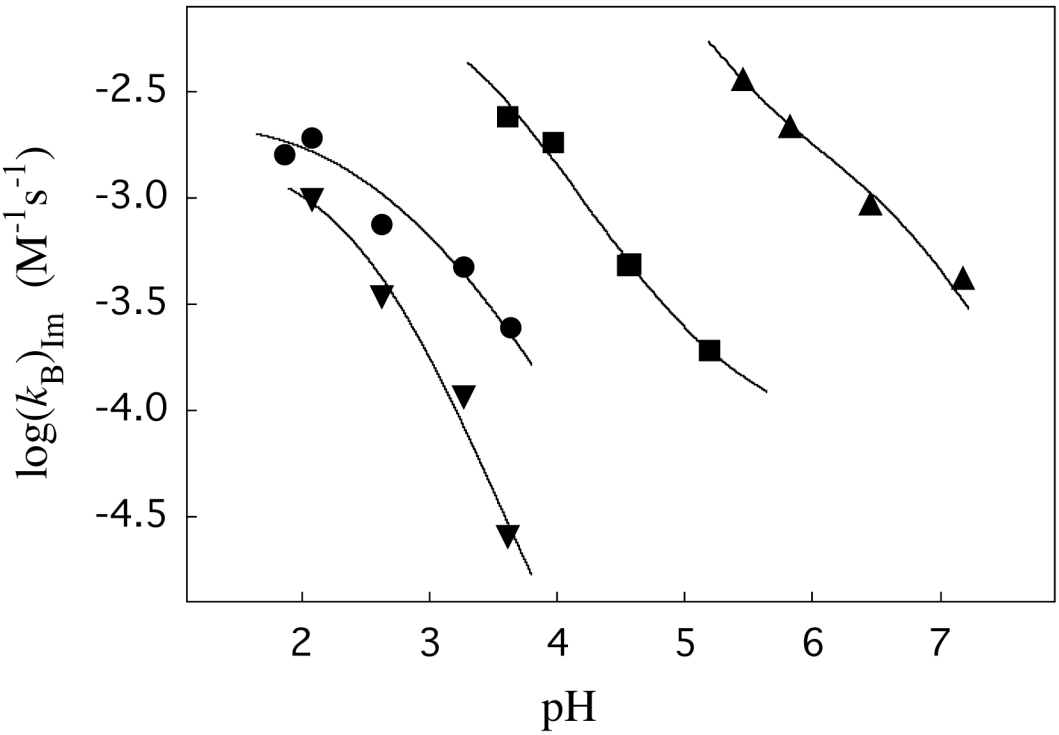

Figure 6.

The pH rate profiles for the second-order rate constants $(k_B)_{Im}$ for the general base-catalyzed deprotonation of **2**. The solid lines show the fits of the experimental data to partial forms of eq 2 determined as described in the text. Key: (▲), phosphate dianion; (■), acetate anion; (●), chloroacetate anion. (▼), glycine zwitterion.

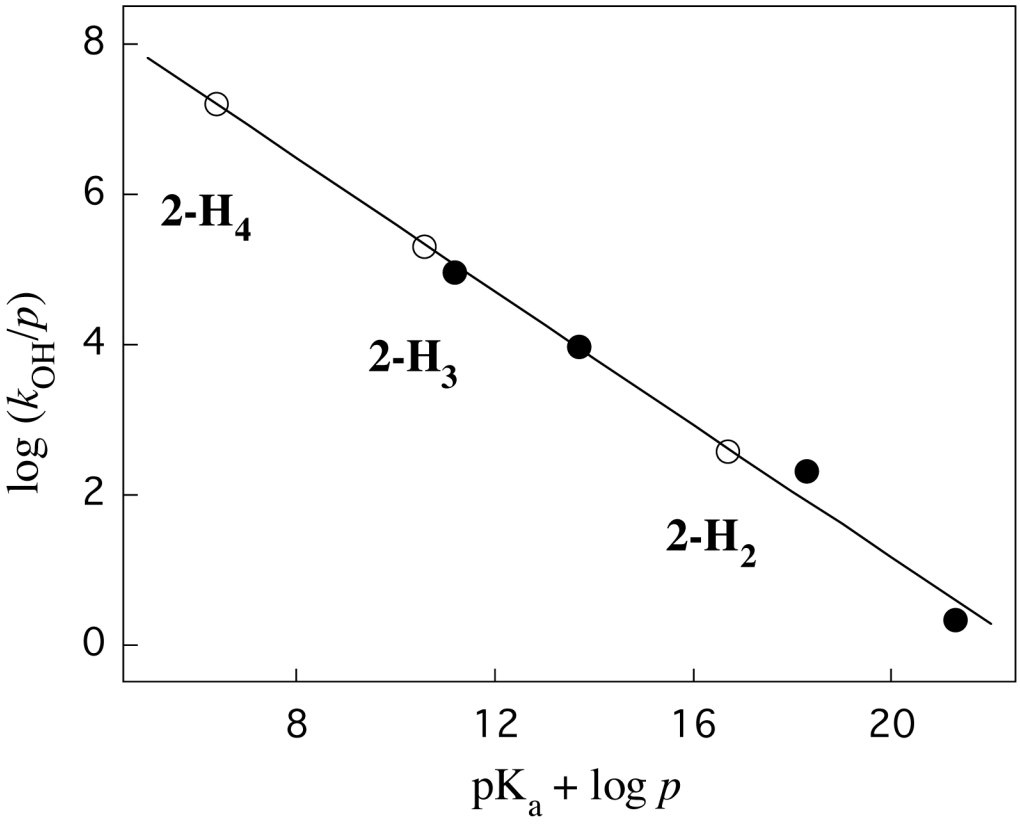

Figure 7.

Brønsted-type relationship between the second-order rate constants for deprotonation of cationic carbon acids by hydroxide ion and carbon acid pK_a, where p is the number of equivalent protons for the carbon acid. The solid circles show data used to define this linear relationship: (carbon acid, pK_a) PyrN^+-CH_2COPh, 10.9; $(CH_3)_2C{=}NH^+CH_2CO_2Me$, 14; $^+Me_3NCH_2CO_2Me$, 18; $^+H_3NCH_2CO_2Me$, 21. The open symbols show the different ionic forms of the pyridoxal-glycine imine (Chart 2). The pK_as of these carbon acids were estimated by making the assumption that values of log (k_{HO}/2) for their deprotonation lie on this linear correlation.

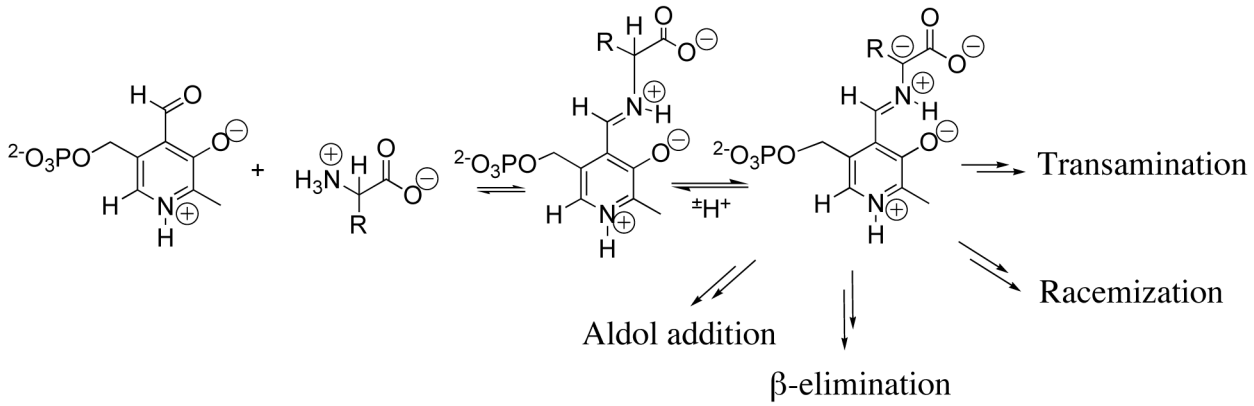

Scheme 1.

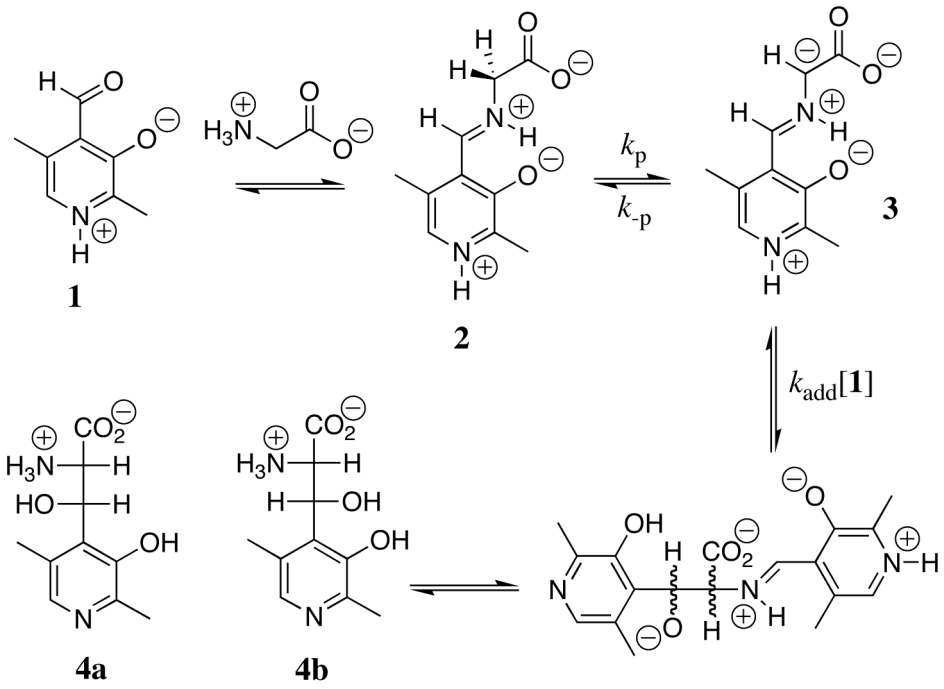

Scheme 2.

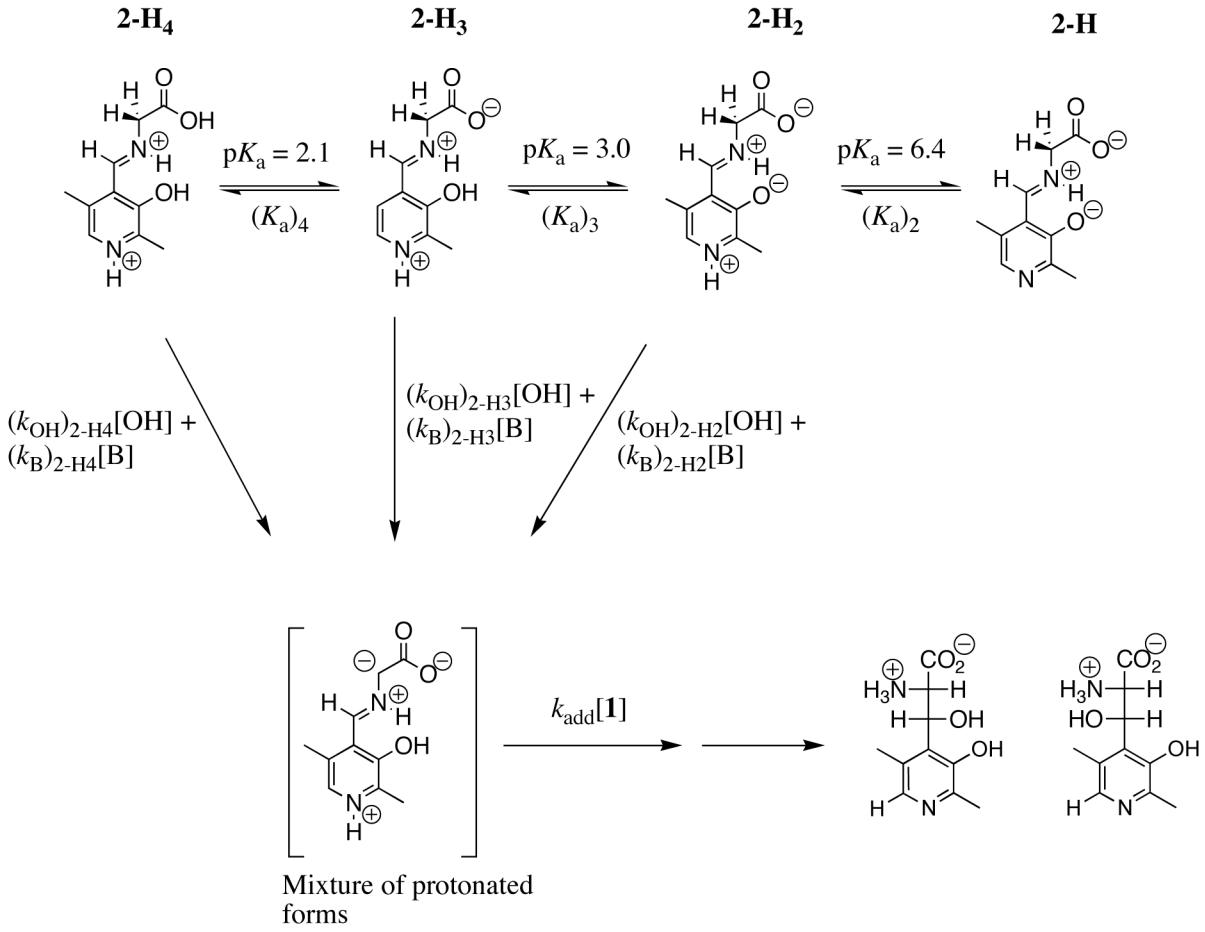

Scheme 3.

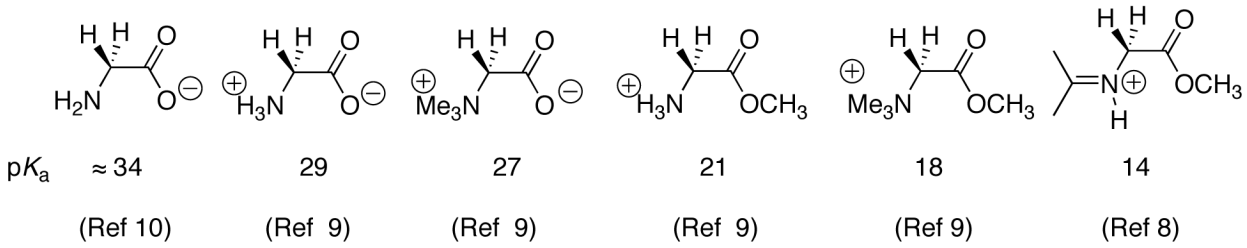

Chart 1.

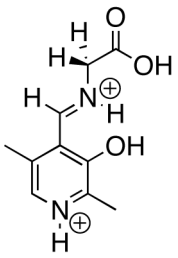

2-H$_4$

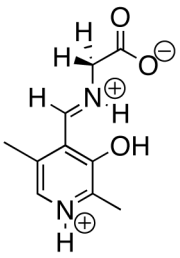

2-H$_3$

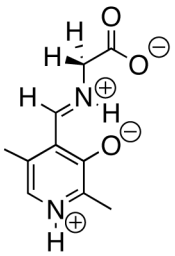

2-H$_2$

pK_a	6	11	17

Chart 2.

Table 1

Kinetic Parameters for Solvent-Catalyzed Claisen-Type Addition of Glycine to **1** (Scheme 2)[a]

pH	Buffer	[glycine]$_T$ (M)	f_{Im}[b]	$(k_0)_{obsd}/10^{-6}$ (s^{-1})[c]	$(k_0)_{Im}/10^{-6}$ (s^{-1})[d]
2.1	Chloroacetate	0[e]			26
		0.050	0.0055[f]	0.20	36
		0.10	0.011	0.61	55
		0.20	0.022[f]	1.6	74
2.7		0[e]			23
		0.050	0.019[f]	0.62	32
		0.10	0.037	1.6	42
		0.20	0.071	4.3	60
3.3		0[e]			24
		0.050	0.062[f]	1.8	29
		0.10	0.12	4.1	34
3.6	Acetate	0[f]			17
		0.10	0.28	5.3	19
		0.20	0.53	11	21
4.0		0.10	0.36	4.7	13
4.6		0.10	0.52	3.7	7.2
5.2		0.10	0.57	3.4	6.0
5.5	Phosphate	0.10	0.58	4.5	7.7
5.9		0.10	0.63	7.0	11
6.5		0.10	0.71	12	17
7.1		0.10	0.84	19	23

[a] For reactions of 10 mM **1** at 25 °C and I = 1.0 (KCl).

[b] The fraction of total **1** that is converted to the imine at the given concentration of glycine determined by NMR analysis of an equilibrium mixture of **1**, **1**-hydrate and the imine, unless stated otherwise.

[c] The observed rate constant for the buffer-independent Claisen addition reaction, determined as the intercept of a plot of k_{obsd} against the concentration of the buffer catalyst.

[d] $(k_0)_{Im} = (k_0)_{obsd}/f_{Im}$.

[e] The intercept of a linear plot of $(k_0)_{Im}$ against $[glycine]_T$.

[f] Calculated from the value of f_{Im} determined for reaction in the presence of 0.10 M glycine by assuming that f_{Im} is directly proportional to the concentration of glycine in the reaction mixture.

Table 2

Kinetic Parameters for General Base-Catalyzed Claisen-Type Addition of Glycine to **1** (Scheme 2)[a]

pH (f_B)[b]	Base Catalyst	[glycine]$_T$ (M)	f_{Im}[c]	$(k_B)_{obsd}$ /10^{-5} ($M^{-1}s^{-1}$)[d]	$(k_B)_{Im}$/10^{-4} ($M^{-1}s^{-1}$)[e]
2.1	Glycine pK_a = 2.5				9.8[f]
2.7					3.4[f]
3.3					1.1[f]
3.6					0.25[f]
2.1 (f_B = 0.20)	Chloroacetate pK_a = 2.7	0.050	0.0055[g]	1.1	20
		0.10	0.011	1.7	15
		0.20	0.022[g]	4.5	21
		Average			19
2.7 (f_B = 0.50)		0.050	0.019[g]	1.3	7.5
		0.10	0.037	2.5	7.7
		0.20	0.071	4.9	6.9
		Average			7.4
3.3 (f_B = 0.80)		0.050	0.062[g]	2.9	4.7
		0.10	0.12	5.5	4.6
		Average			4.7
3.6 (f_B = 0.10)	Acetate pK_a = 4.6	0.10	0.28	69	25
		0.20	0.53	120	23
		Average			24
4.0 (f_B = 0.20)		0.10	0.36	65	18
4.6 (f_B = 0.50)		0.10	0.52	25	4.9
5.2 (f_B = 0.80)		0.10	0.57	11	1.9
5.5 (f_B = 0.10)	Phosphate pK_a = 6.5	0.10	0.58	210	36
5.9 (f_B = 0.20)		0.10	0.63	140	22
6.5 (f_B = 0.5)	Phosphate	0.10	0.71	67	9.4
7.1 (f_B = 0.20)		0.10	0.84	35	4.2

[a] For reactions of 10 mM **1** at 25 °C and I = 1.0 (KCl).

[b] Fraction of the buffer in the basic form.

[c] [b] The fraction of total **1** that was converted to the imine at the given concentration of glycine, determined by NMR analysis of an equilibrium mixture of **1**, **1**-hydrate and the imine unless stated otherwise.

[d] The observed second-order rate constant for general base-catalyzed Claisen-type addition of glycine to **1** determined as the slope of a plot of k_{obsd} against the concentration of the basic form of the buffer.

[e] $(k_B)_{Im} = (k_B)_{obs}/f_{Im}$ except for the glycine-catalyzed reactions.

[f] The slope of replots of the type shown in the inset of Figure 4 for the reaction at pH 2.7

[g] Calculated from the value of f_{Im} determined for reaction in the presence of 0.10 M glycine by assuming that f_{Im} is directly proportional to the concentration of glycine in the reaction mixture.

Table 3

Second-order Rate Constants for Deprotonation of Different Ionic Forms of **2** by Hydroxide Ion and Buffer Bases[a]

Base	pK_a[b]	$(k_B)_{2\text{-}H4}$ ($M^{-1}s^{-1}$)[c, d]	$(k_B)_{2\text{-}H3}$ ($M^{-1}s^{-1}$)[c, e]	$(k_B)_{2\text{-}H2}$ ($M^{-1}s^{-1}$)[c, f]
OH^- [b]	15.7	3.0×10^{7}	3.8×10^{5}	7.5×10^{2}
HPO_4^{2-}	6.5		4.3×10^{-1}	1.7×10^{-3}
CH_3COO^-	4.6		1.1×10^{-2}	1.0×10^{-4}
CH_2ClCOO^-	2.7	2.3×10^{-3}	8.2×10^{-4}	
$NH_2CH_2COO^-$	2.1	1.6×10^{-3}	4.5×10^{-5}	

[a] For reactions of 10 mM **1** at 25 °C and I = 1.0 (KCl).

[b] Calculated from the solution pH and the ratio of the acidic and basic forms of the buffer under our experimental reaction conditions.

[c] Rate constants determined from the fit of the experimental data to eq 1 derived for Scheme 2 as described in the text.

[d] Rate-constants for buffer-catalyzed deprotonation of **2-H4**.

[e] Rate-constants for buffer-catalyzed deprotonation of **2-H3**.

[f] Rate-constants for buffer-catalyzed deprotonation of **2-H2**.